Accepted Manuscript

Title: Artificial biomembranes stabilized over spin coated hydrogel scaffolds. Crosslinking agent nature induces wrinkled or flat surfaces on the hydrogel.

Author: C.M. González-Henríquez G.C. Pizarro-Guerra E.N. Córdova-Alarcón M.A. Sarabia-Vallejos C.A. Terraza-Inostroza

PII: S0009-3084(16)30004-4
DOI: http://dx.doi.org/doi:10.1016/j.chemphyslip.2016.02.001
Reference: CPL 4448

To appear in: *Chemistry and Physics of Lipids*

Received date: 30-10-2015
Revised date: 13-1-2016
Accepted date: 2-2-2016

Please cite this article as: González-Henríquez, C.M., Pizarro-Guerra, G.C., Córdova-Alarcón, E.N., Sarabia-Vallejos, M.A., Terraza-Inostroza, C.A., Artificial biomembranes stabilized over spin coated hydrogel scaffolds.Crosslinking agent nature induces wrinkled or flat surfaces on the hydrogel.Chemistry and Physics of Lipids http://dx.doi.org/10.1016/j.chemphyslip.2016.02.001

Artificial biomembranes stabilized over spin coated hydrogel scaffolds. Crosslinking agent nature induces wrinkled or flat surfaces on the hydrogel.

C.M. González-Henríquez[a,b]*, G.C. Pizarro-Guerra[a], E.N. Córdova-Alarcón[a], M.A. Sarabia-Vallejos[c], C.A. Terraza-Inostroza[d].

[a]Departamento de Química, Universidad Tecnológica Metropolitana, Las Palmeras # 3360, P.O. Box 7800003, Santiago, Chile

[b]Programa Institucional de Fomento a la Investigación, Desarrollo e Innovación, Universidad Tecnológica Metropolitana, Las Palmeras #3360, P.O. Box 7800003, Santiago, Chile

[c]Instituto de Física, Pontificia Universidad Católica de Chile, Avda, Vicuña Mackenna #4860, P.O. Box 7820436, Santiago, Chile

[d]Facultad de Química, Pontificia Universidad Católica de Chile, Avda, Vicuña Mackenna #4860, P.O. Box 7820436, Santiago, Chile

*Corresponding author.

Graphical abstract

Highlights

- Hydrogel films, deposited through spin coating technique, were used as scaffold for artificial biomembranes.
- DPPC bilayer (artificial membrane model) was deposited over hydrogel films using Langmuir-Blodgett technique.
- Wrinkled or flat surfaces were spontaneously formed in the top of hydrogel layers according to crosslinking agent nature.
- DPPC phase and phase transitions were detected using ellipsometry and AFM techniques.
- Hydrogel-cushioned biomembranes maintain their stability in time under uncomfortable conditions.

ABSTRACT

Hydrogel films possess the ability of retain water and deliver it to a phospholipid bilayer mainly composed by DPPC (1,2-dipalmitoyl-*sn*-glycero-3-phosphocholine); moisture of the medium favors the stability of an artificial biomembrane when it is subjected to repetitive heating cycles. This hypothesis is valid when the hydrogel film, used as scaffold, present a flat surface morphology and a high ability for water releasing. On the other hand, when the sample presents a wrinkle topography (periodic undulations), free lateral molecular movement of the bilayer becomes lower, disfavoring the occurrence of clear phases/phase transitions according to applied temperature.

Hydrogel films were prepared using HEMA (hydroxyethylmetacrylate), different crosslinking agents and initiators. This reaction mixture was spread over hydrophilic silicon wafers using spin coating technique. Resultant films were then exposed to UV light favoring polymeric chain crosslinking and interactions between hydrogel and substrate; this process is also known to generate tensile stress mismatch between different hydrogel strata, producing out-of-plane net force that generate ordered undulations or collapsed crystals at surface level. DPPC bilayers were then placed over hydrogel using Langmuir-Blodgett technique. Surface morphology was detected in order to clarify the behavior of these films. Obtained data corroborate DPPC membrane stability making possible to detect phases/phase transitions by ellipsometric methods and Atomic Force Microscopy due to their high hydration level. This system is intended to be used as biosensor through the insertion of transmembrane proteins or peptides that detect minimal variations of some analyte in the environment; artificial biomembrane stability and behavior is fundamental for this purpose.

Keywords: Tethered lipid membranes; Polymer scaffolds; Bilayer phase transitions; Wrinkled

patterns; Ellipsometry

- **Introduction.**

Tethered bilayer lipid membranes (tBLMs) have attracted large interest from current and modern research in the biotechnology field due to their wide application in technology development for tissue engineering, drug delivery, biosensors and protein channel transduction, among others (Drücker et al., 2014). Supported lipid bilayers (SLBs) is the most common and widely used configuration of tBLMs, corresponding to planar membranes deposited onto hydrophilic solid substrates separated with an ultrathin film of water (1–2 nm) (Rebaud et al., 2014). Thermal studies of these systems elucidate the behavior and properties of cell membranes, and - also - the efficiency of possible devices based on SLBs when are subjected to temperatures near ambient. In this way, the determination of bilayer phase/phase transition temperatures becomes in relevant information (Thiam et al., 2013). Some characterization techniques as magnetic resonance, Raman spectroscopy, atomic force microscopy has been utilized for this purpose (Shlomovitz and Schick, 2013; Hain et al., 2013) allowing the detection of minimal structural changes in bilayer conformation such as thickness, smooth/roughness, molecule tilting and electric interaction between phospholipids (Jing et al., 2014). However, the complexity of SLBs systems lies in the low structural stability of the bilayer during formation processes and posterior characterization (Andrecka et al., 2013). In order to solve this problem, scaffolds for tBLMs are frequently used; the compound utilized as support must maintain an aqueous (moist) environment that increase their stability during long periods, particularly in unusual conditions (high temperatures, pressure variations, external

mechanical stress and pH changes) (Luckey, 2014).

Polymer scaffolds enhance surface-bilayer interactions compared to several others materials commonly used such as aluminium, titanium, iron and silicon oxides (Nellis et al., 2011). Hydrogel is a kind of polymer, which has the capacity to absorb and retain large amounts of solvents into their structural network, being an excellent candidate for membrane support without direct linkage, significantly reducing the frictional coupling between membrane and solid substrate acting as "lubricant cushion" for the interface (Rebaud et al., 2014).

In this study, 1,2-dipalmitoyl-*sn*-glycero-3-phosphocholine (DPPC) was used for bilayer formation. This pulmonary surfactant present three characteristic phases; subgel (L_c), gel (L_β) and liquid crystalline (L_α) with their respective transitions: laminar gel ($L_{\beta'}$) and ripple gel ($P_{\beta'}$), the superscript of prime means that lipid molecules are oriented tilted from the bilayer plane (Matsuki et al., 2013).

Different types of photo-polymerized hydrogel films, based on polyhydroxyethylmetacrylate (pHEMA), were used as scaffold for DPPC. The technique used to deposit the hydrogel was spin coating, producing a high surface homogeneity; posteriorly, the compounds were exposed to UV light (λ = 365 nm) in order to complete the polymerization. The systems formed by DPPC/Hydrogel films/Silicon wafer were characterized through different methods. Hydrogel film surface was analyzed using Field Emission gun Scanning Electron Microscopy (FE-SEM) in order to visualize the surface morphology. Atomic Force Microscopy (AFM) was used to detect surface structures dimensions and profiles. Simultaneously, heating cycles were applied during these measurements in order to obtain micrographies at different temperatures, this data was then used to calculate surface roughness for

identification of DPPC phases with their respective transitions. Ellipsometric measurements were realized in every deposition step in order to obtain an appropriate thickness control, also, DPPC thickness variations were measured against temperature in order to corroborate phases and phase transitions temperatures detected via AFM.

Different surfaces morphologies were obtained according to the hydrogel type utilized as scaffold (undulated pattern in some cases or flat surface with some crystals structures in others). Patterns morphology and their dimensions are related to the ratio between monomer and crosslinking agent, to the polymerization technique utilized and with the deposition method, these processes generate a stress gradient between film surface and lower strata (Guvendiren et al., 2010). When hydrogel film show tightens wrinkles, DPPC bilayer is found highly packaged affecting their molecular mobility, disfavoring phase (transitions) occurrence. On the other hand, flat topography is ideal for detect thermal behavior of the surfactant and for conserve membrane stability during thermal cycles.

- **Materials and Methods.**

- *Materials.*

For hydrogel synthesis, the following precursors were utilized: 2-hydroxyethyl methacrylate (HEMA, 97 %) containing monomethyl ether hydroquinone as inhibitor (≤ 250 ppm) as main monomer. Four different crosslinking agents were employed: Di (ethylene glycol) dimethacrylate (DEGDMA, ≥ 95 %) that includes monomethyl ether hydroquinone as inhibitor (300 ppm). Poly(ethylene glycol) diacrylate (PEGDA), with two different average molecular weights (Mn: 575 and 700 g/mol) and Acrylamide (AAm, ≥ 99 %) for molecular biology applications (HPLC purity). 2-hydroxy-4′-(2-

hydroxyethoxy)-2-methylpropiophenone (Irgacure 2959, 98 %) and 2,2-dimethoxy-2-phenylacetophenone (Irgacure 651, 99 %) were utilized as photo-initiators, all the reagents previously mentioned were purchased from Sigma-Aldrich (St. Louis, Missouri, USA). Pre-polymer (oligomer) was synthesized using ACS ammonium peroxodisulfate (98 %, grade reagent) as thermal initiator. 1-vinyl-2-pyrrolidone (NVP, stabilized with N,N´-di-sec-butyl-1,4-phenylenediamine) was employed for dissolve the photo-initiator; both reagents were acquired from Merck KGaA (Darmstadt, Germany).

1,2-Dipalmitoyl-*sn*-glycero-3-phosphocholine (DPPC, ≥ 99 %, powder) was acquired from Sigma-Aldrich Company (St. Louis, Missouri, USA) and used without further purification, while chloroform (99.0-99.4 %), hydrogen peroxide (30-32 %), sulfuric acid (95-97 %) Emparta®ACS and Water for chromatography LiChrosolv® were obtained from Merck KGaA (Darmstadt, Germany). A *p* type <100> ±0.5º orientation silicon wafer was acquired from Siegert Wafer GmbH (Aachen, Germany).

- *Equipment and Measurements.*

Hydrogel polymerizations were performed through UV exposure using a lamp with its emission peak centered at λ = 365 nm (Vilber Lourmat 230V 50/60Hz, 9W). A KW-4A spin coater (Chemat Scientific), coupled with an oil free vacuum pump (Rocker Chemker 410), was utilized for deposit hydrogels on hydrophilic silicon wafer. DPPC bilayer deposition, with hydrogel film used as scaffold, was performed with a Langmuir-Blodgett trough model LT-103 (MicroTestMachines).

Micrographies of HEMA-DEGDMA films were obtained with two different high resolution FE-SEM models, JSM 6330 F (JEOL Ltd.) and Quanta FEG 650 (FEI Co.),

at different magnifications (1000x and 5000x).

The samples that possess a DPPC bilayer on the top, were analyzed using an atomic force microscope (AFM), model NX10 (Park Systems), height profiles of the surfaces were obtained with a scan width of 20×20 μm^2 and with a super-sharp silicon probe (10 nm radius, 330 kHz resonance frequency and spring constant of 42 Nm^{-1}), this AFM possess a sample heater that permits to increase the temperature between ambient and 60 °C; the equipment is located at Brazilian Nanotechnology National Laboratory (LNNano) in Campinas, Brazil. The topographies of HEMA-$PEGDA_{575}$ and HEMA-$PEGDA_{700}$ were obtained at room temperature using another AFM, model NTEGRA Prima (NT-MDT Co.) in intermittent contact mode using a tips of 75 kHz resonance frequency. Images were treated using the off-line software packages Gwyddion (Klapetek et al., 2011) and WSxM 4.0/8.0 (Horcas et al., 2007) for qualitatively and quantitatively analyze the acquired images.

A Multi-angle laser ellipsometer model SE 400adv (SENTECH Instrument GmbH) was used to perform optical measurements, the equipment possesses a stabilized He-Ne laser (λ = 633 nm). This instrument was used in conjunction with a home-made copper sample holder coupled with a temperature controller model 325, a Pt100 sensor (model PT-102-2S, useful range 1.4 K to 873 K) and a 25 Watt heater (model HTR-25), all acquired from Lake Shore Cryotronics Inc.; this close-loop system permits the regulation and stabilization of sample temperature between 25 °C and 70 ° C.

- *Sample Preparation.*

Firstly, the substrates were treated for generate a hydrophilic surface using a piranha solution composed by H_2SO_4:H_2O_2 (7:3 vol/vol ratio) during 30 minutes at 80 °C.

Afterwards, they were washed and dried with an ultra-pure nitrogen gas jet (Tidswell et al., 1990). This method removes native silicon oxide layer and generate a new layer of SiO_2 with thickness near to 2.1 nm that possess a low contact angle (< 10 º).

- *Hydrogel synthesis.*

All hydrogels were prepared in transparent flasks covered with a septum according to the following procedure:

a) HEMA-DEGDMA*:* 1 g of HEMA (7.68 mmol), 18.95 mg of DEGDMA (0.078 mmol), 0.5 mL of water, 9.07 mg of ammonium peroxodisulfate (0.039 mmol) and 18.22 mg of Irgacure 651 (0.071 mmol) (González et al., 2014a).

b) HEMA-$PEGDA_{575/700}$*:* 1 g of HEMA (7.68 mmol), 1.5 g of PEGDA (Mn 575/700, 2.61/2.14 mmol), 0.625 mL of water, 10.0 mg of ammonium peroxodisulfate (0.0766 mmol) and 17.49 mg of Irgacure 2959 (0.0779 mmol). This last compound was dissolved in 0.1 mL of NVP (González et al., 2014b).

c) HEMA-AAm: 1 g of HEMA (7.68 mmol), 60.68 mg of AAm (0.85 mmol), 0.5 mL of water, 8.76 mg of ammonium peroxodisulfate (0.038 mmol) and 19.68 mg of Irgacure 651 (0.076 mmol).

The reaction mixtures were continuously purged with nitrogen gas in order to displace the air from the system avoiding unnecessary oxidation. The flasks were then placed in an oil bath at 50 °C for trigger the thermal pre-polymerization (oligomer formation); this heating process produces a slight increase in density and viscosity of the solution, producing a larger and homogeneous coverage of the oligomeric film over the substrate using spin coating as deposition technique.

- *Film deposition using spin coating technique.*

10 µL of the oligomeric solution was placed on the center of the silicon wafer (1×1 cm^2) with posterior spinning at 6000 rpm during 60 seconds. The samples were then irradiated with an UV lamp (λ = 365 nm) during 1 hour for complete the polymerization.

- *DPPC bilayer over spin coated hydrogel films.*

The sample should be initially immersed into sub-phase (water) before start the deposition using the following procedure: 1 mg of phospholipid was dissolved in 0.5 mL of chloroform. Then this solution was spread drop by drop with a Hamilton syringe (60 µL of solution) over a pure water interface (Langmuir-Blodgett trough) at constant room temperature (25 °C). Secondly, the compression procedure was initiated at ~1.5 mm/seconds generating DPPC monolayer formation into air-water interface. Compression arm moves at this velocity until reach proper surface pressure for deposition (45.8 mN/m, obtained through isotherm analysis) (Watkins et al., 2014). At this moment, phospholipid head groups interacts with hydrophilic hydrogel surface producing first monolayer deposition via contact adhesion process by move the substrate upwards slowly at 0.01 mm/s. Subsequently, the second monolayer was transferred through substrate immersion at same speed. Finally, in order to avoid a third monolayer deposition, the barrier is moved to the original position for DPPC remotion from the interface. This procedure ensures a homogeneous Y-type bilayer formation for each sample.

- **Results and discussion**

After hydrogel film photo-polymerization it is necessary to place the sample into rough vacuum (10^{-3} torr) during 3 hours in order to remove water (deswelling) that is

trapped between polymer network spaces. According to the crosslinking agent used in the synthesis, different morphologies can be achieved, surface homogeneity (appropriate for ellipsometric measures) in some cases, and buckling in others. Wrinkled topography is generated due to deswelling process that induces a stress gradient between film surface and the layers underneath (Hou et al., 2014; Tokudome et al., 2012), water deswelling induce a mayor volume contraction of the top strata; surface buckling of this hydrogel could be observed via different kind of microscopy techniques like FE-SEM and AFM. It should be noted that the hydrogel thickness (multilayer) was obtained via ellipsometric techniques, resulting in values between 240-280 nm.

Finally, it is important to mention that the characterization of the samples (FE-SEM, AFM and Ellipsometry) was performed in triplicate, the average of these studies, with their respective standard deviation, or representative images are showed in this section.

- *Field Emission Scanning Electron Microscopy (FE-SEM).*

As described above, different hydrogels using HEMA (as base monomer) and DEGDMA, $PEGDA_{575}$, $PEGDA_{700}$ and AAm (as crosslinking agents) were used to prepare films by spin coating technique. These multilayers act as support (polymer-cushioned scaffold) for DPPC bilayer, producing enough humectation in their environment, enhancing membrane stability and avoiding phospholipid denaturation. The surface morphologies were studied by FE-SEM in order to visually recognize the structures formed at the top of the samples. In Figures 1-3 it is possible to detect different morphologies according to the type of crosslinking agent used during the hydrogel synthesis. In some cases, crystalline morphology (lamellar or regular

structures) over flat and smooth film background were recognized, and in other cases, homogeneous rugged and ordered wrinkled patterns without clusters or crystalline structures were visualized.

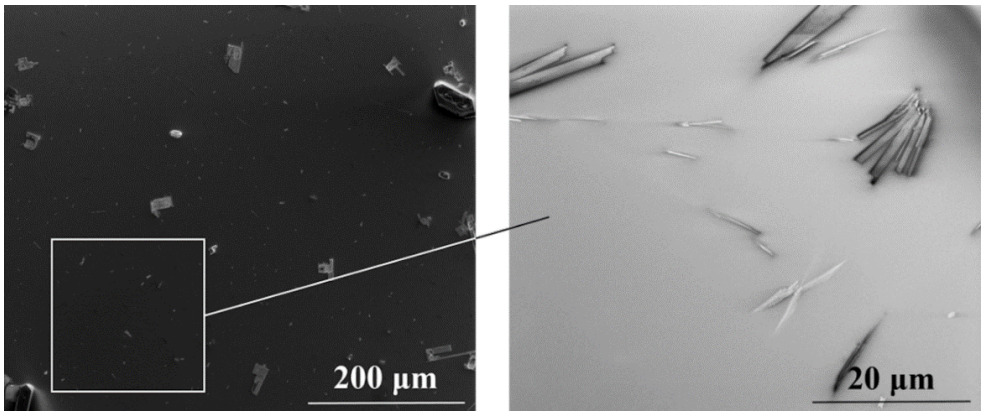

Figure 1. Surface topography for HEMA-DEGDMA hydrogel films using FE-SEM at two different magnifications; 1000x (right) and 5000x (left).

Figure 1, exhibits flat film at background with some crystals isolated at surface with variable sizes, two different groups of crystals can be defined according to their size and morphology, rod- and square-like shaped micro-crystals. The same sample was observed in different sectors (using the same magnification) in order to corroborate surface homogeneity. All the samples were fabricated and measured in triplicate for demonstrate reproducibility. Using this data, it was possible to measure crystal dimensions (large and width), obtain their corresponding standard deviation and

corroborate the integrity of the data for each case; F- and t-tests demonstrate that null hypothesis is valid for several sectors of the different samples, indicating that the large and width, independently, statistically belongs to the same population (- t-value Two-tails < t-value Stat. < t-value Two-tails). Thus, the rod-like crystals present dimensions of: 6.92 ± 2.62 μm (large) and 0.86 ± 0.47 μm (width), this sample also presents small square-like crystals with dimensions of: 5.78 ± 0.91 μm (large) and 3.07 ± 0.49 μm (width). These structures could be related to the PEG part of DEGDMA, generating an arrangement of the hydrophilic regions (ethylene oxide groups) that probably produce the formation of lamellar crystalline organizations (Stiebler et al., 2010). However, these micrographs reveal polymeric films with apparent homogenous morphology at the background, demonstrating high miscibility between the two monomers used for hydrogel formation (HEMA and DEGDMA). In order to corroborate this hypothesis, EDS measurements were performed in background sector detecting low atomic presence of silicon (~ 6 %, due to substrate used) and high atomic presence of organic phase, mainly carbon and oxygen (~ 92 % in total); also small quantities of metallic materials like copper, iron or aluminum (~ 2 %) were found due to traces present in the reactive used. EDS of surface faceted structures (rod- and square-like) demonstrate that their composition is completely organic (~ 99 % of C and O, and ~ 1 % of other metallic traces). Likewise, the presence of these structures at surface level is an indicator that the formation of homogeneous layers using this type of hydrogel is a very difficult task.

Figure 2 shows a surface texture completely different to that shown in Figure 1. Thus, the incorporation of PEGDA into reaction mixture favor rough surface formation that present an interesting wrinkle topography. Thus, UV film irradiation, the high

proportion of PEG and their molecular weight could be some of the parameters responsible of generate tensile instability of the film at surface level, producing spontaneous layer contractions leading to wrinkles and folds formation. In these films, the photo-polymerization degree of the mixture diminishes according to sample depth, producing a crosslink gradient related to UV light absorption. This phenomenon generates a slight strain mismatch between neighbor layers, forming structural instabilities and deformations that travels through the film until reach the surface and finally producing the undulations visualized in Figure 2. The presence of a rigid support enhances the gradient of stress forces between top and underneath layers. Thus, these microstructures commonly occur when the in-plane compressive strain exceed critical values, leading to out-of-plane periodic undulations of self-layered structures (Kim et al., 2014; Palacios-Cuesta et al., 2014).

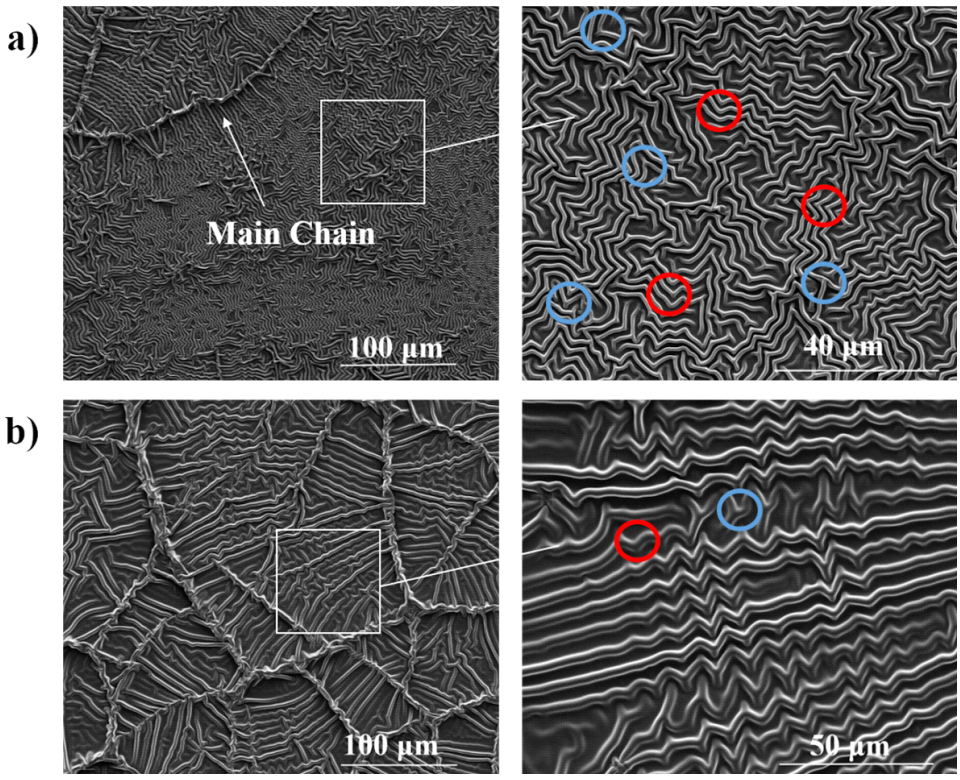

Figure 2. Film surface topography detected via FE-SEM of hydrogel films at different magnifications: a) HEMA-PEGDA$_{575}$ and b) HEMA-PEGDA$_{700}$.

In this wrinkle architecture it is possible to detect hydrogel chain braiding resulting in a

repetitive and homogeneous network with some hierarchy structuration; mainly represented by significant and relatively abrupt changes in the size and ordering of the wave pattern. Thus, HEMA-PEGDA$_{575}$ films show a disordered chain buckling (non-preferential wrinkles orientation) at surface level; this system presents a wider visible main chain rounded by smaller chains connected to the main one (Figure 2a). The small secondary chains present a wavelength that varies between ~ 2.5 – 2.9 µm with a mean located at ~ 2.67 ± 0.24 µm; the main chain present a width mean of ~ 4.31 ± 0.47 µm (~ 4.2 – 4.5 µm).

Additionally, some particular and identifiable defect types can be visualized following two self-organized patterns (right images with higher magnifications); disclinations (blue circles) and edge dislocations (red circles), defects that are product of surface instabilities mentioned above (Huang, 2005). The first type (disclinations) could be identified as a wrinkle division into three different ones homogeneously separated by similar angles (~120°) that could be probably explained via point defects present in hydrogel film structure. Edge dislocations can be identified as spontaneous variation in wrinkle direction. This surface behavior is mainly related with wrinkle growth evolution process and therefore with natural or intrinsic properties of the polymer mixture (Kim et al., 2014).

On the other hand, the dimensions of the chains of HEMA-PEGDA$_{700}$ (Figure 2b) are in general larger than the chains detected for PEGDA$_{575}$. These junctions have a certain periodicity in their structuration; secondary chains exhibited a mean wavelength of 3.48 ± 0.42 µm, this chains are oriented parallel with respect to each other, while main chains, from where secondary ones are originated, present a mean width of 5.78 ± 0.47 µm. This data (PEGDA$_{575}$ and PEGDA$_{700}$) was also verified via statistical

methods (F- and t-tests) in order to corroborate that null hypothesis ($\mu_1 = \mu_2$) is valid for different sectors of the sample, indicating that the surface is homogeneous, also statistical tests were performed to check that mean values of the width of main and secondary chains correspond to different populations.

Therefore, PEGDA molecular weight is fundamental for predict film morphology. As mentioned above, PEGDA hydrogel presented a quite interesting surface wave structure, which produce an increase in their contact area; hence, this finding was interesting for applications in several technological fields, particularly in where the surface ruggedness is important such as microfluidic devices, drug delivery, tissue engineering, among others.

HEMA-AAm hydrogel films (Figure 3) were also studied by FE-SEM and reveal similar topography compared to HEMA-DEGDMA films (Figure 1), where a smooth and flat background hydrogel surface could be visualized. EDS measurements were consistent with this observation, with similar composition values compared with HEMA-DEGDMA films. Likewise, crystalline structures (rod- and square-like) were detected over film surface; square-like crystals with dimensions of ~ 13.83 ± 3.67 μm (large) and ~ 12.51 ± 2.04 μm (width) were detected, also rod-like crystals were visualized and present dimensions of ~ 4.16 ± 0.21 μm (large) and ~ 2.53 ± 0.19 μm (width). Amorphous copolymers (amphiphilic block), formed by both flexible and rigid groups from HEMA and AAm structures, could benefit the orientated growth of this regular structures isolated at the surface of the film.

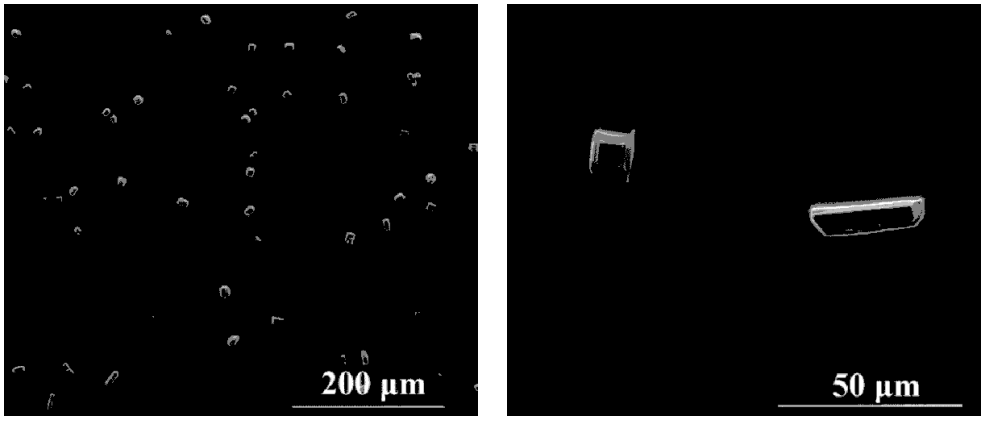

Figure 3. Surface topography for HEMA-AAm hydrogel films using FE-SEM at different magnifications.

As summary, the wrinkle formation at surface is produced when PEGDA is used as crosslinking agent, the evolution of the pattern is related to remnant stresses that generate instabilities between different strata of the film; the morphology of the undulations was found to be dependent on the equilibrium of the material expansion during deposition and photo-polymerization, which is affected by the crosslinking density of network (polymer) together with material behavior under this conditions (Guvendiren et al., 2010). When DEGDMA and AAm were used as crosslinking agents, a flat background with isolated crystals are visualized. The FE-SEM results, previously mentioned, are summarized in two different tables (Table 1 and 2) and compared with AFM results in the next section.

- *Atomic Force Microscopy (AFM).*

Micrographies for the mentioned hydrogels with their corresponding height profiles are showed in Figure 4. Additionally, surface roughness (R_a) variation for the sample DPPC/HEMA-AAm was determined when it is exposed to thermal cycles (Figure 5). Thus, thermo-AFM analysis proved that the artificial membrane had detectable phases and phase transitions - phenomenon described and discussed extensible through ellipsometry results.

Height profiles were extracted from AFM micrographies; these results show that surface wrinkles produce an organized pattern with a relative periodical behavior. Thus, HEMA-$PEGDA_{575}$ film shows regular undulations that can be divided into main and secondary chains. The first ones with average wave amplitude of ~ 0.95 ± 0.13 µm and average wavelength of ~ 4.68 ± 0.36 µm, secondary chains present an amplitude of ~ 0.56 ± 0.12 µm and a wavelength of ~ 2.35 ± 0.31 µm (Figure 4b and 4f). Similar topographic periodicity has been detected for the sample HEMA-$PEGDA_{700}$, main chain presents an average wave amplitude of ~ 1.31 ± 0.20 µm and wavelength of ~ 6.05 ± 0.69 µm, secondary chain has an average wave amplitude of ~ 0.88 ± 0.11 µm and wavelength of ~ 3.16 ± 0.71 µm (Figure 4c and 4f). The difference in the amplitude and wavelength between PEGDA samples wrinkled pattern is probably related to crosslinking agent nature (molecular weight) that produces an important increase in both parameters (more than 50 % for HEMA-$PEGDA_{700}$ compared with HEMA-$PEGDA_{575}$).

Height profiles were extracted from several distinct points for each hydrogel sample in order to ensure an appropriate statistical study. Thus, HEMA-DEGDMA and HEMA-

AAm show two different kind of structures in FE-SEM images, rod- and square-like crystals (Figures 1 and 3). Using AFM technique, it was difficult to measure rod-like crystals, probably due to their height; on the other hand, several micrographies and their respective topographic profiles were obtained for square-like crystals for compounds HEMA-DEGDMA and HEMA-AAm, with dimensions of ~ 5.27 ± 0.46 µm (large), ~ 2.56 ± 0.31 µm (width) and ~ 0.33 ± 0.03 µm (height) for HEMA-DEGDMA (Figures 4a and 4e). For HEMA-AAm sample (Figures 4d and 4e) the dimensions were: ~ 3.84 ± 0.20 µm (large), ~ 2.69 ± 0.14 µm (width) and ~ 0.32 ± 0.02 µm (height). Their long/width is similar than measured with FE-SEM technique except for square-like crystals in HEMA-AAm samples, in where the dimension measured through AFM is considerably lower; is important to note that the height of the crystals in both cases is barely the same and do not depend on the crosslinking agent used; these samples present a smooth background under the crystals probably due to the high concentration of HEMA into the reaction mixture.

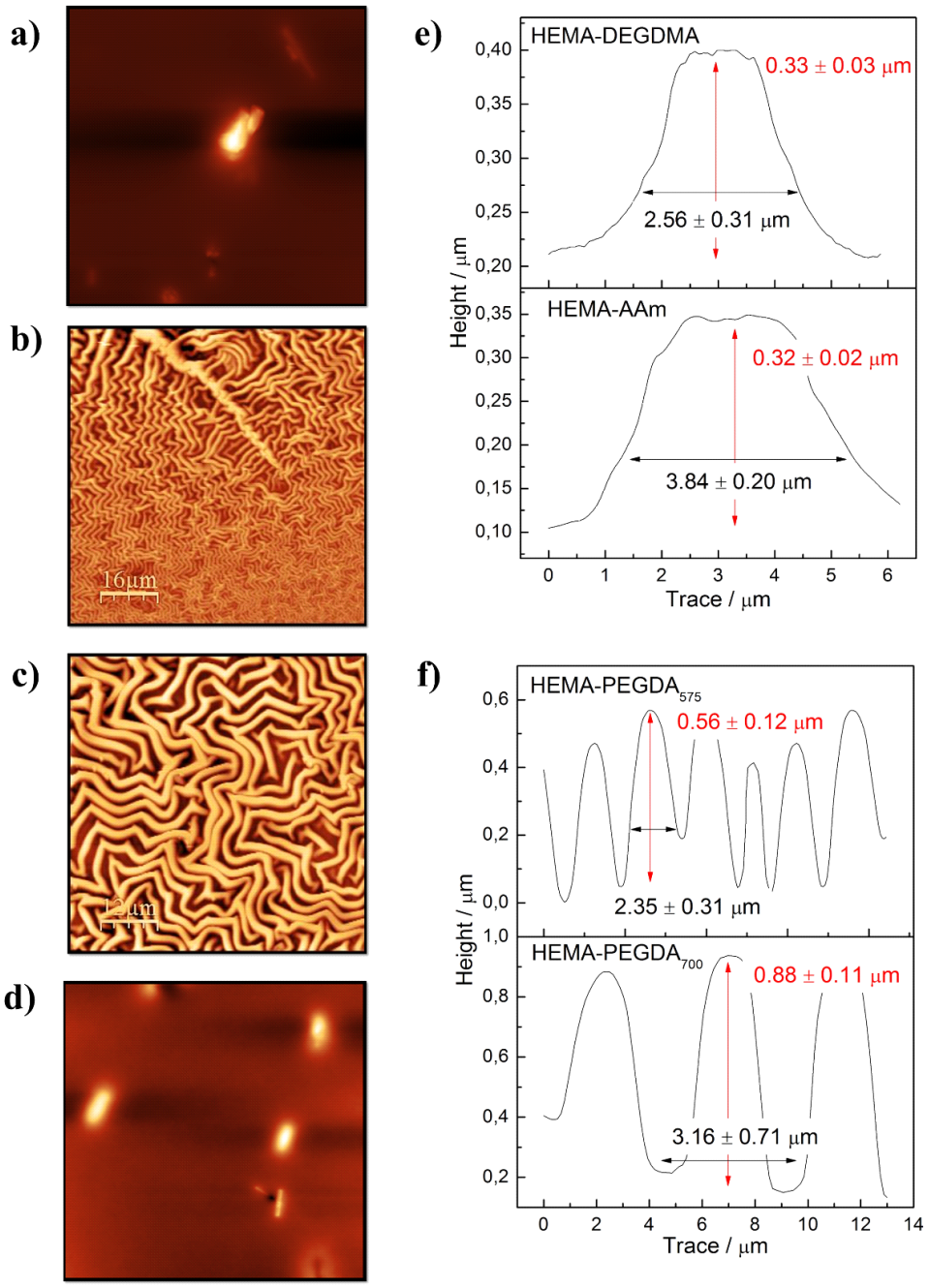

Figure 4. AFM micrographies of: a) HEMA-DEGDMA, b) HEMA-PEGDA$_{575}$, c) HEMA-PEGDA$_{700}$ and d) HEMA-AAm with their respective profiles: e) DEGDMA and AAm crystals and f) PEGDA$_{575/700}$ wrinkles.

AFM micrographies allow to measure roughness changes that permit to identify DPPC phases and transitions due to bilayer surface ordering and molecule tilting, factor that directly depends on applied temperature. Roughness stabilizations correspond to defined and stable bilayer phases; abrupt roughness changes correspond to phase transitions. In order to avoid clusters or wrinkles, that produce an intrinsic roughness that is not related to DPPC ordering, ten squares of 0.1 x 0.1 μm^2 were selected arbitrarily in different zones of the sample; only on these areas the roughness was determined, then the average and standard deviation of these values are showed in Figure 5, the dashed lines in the plot correspond to the statistically calculated limits of the range for the confidence interval at 95 %. This range was determined according to the application of two-tail t-test.

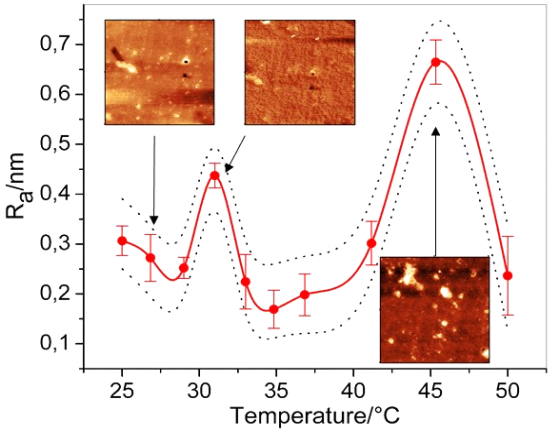

Figure 5. Surface roughness variation of the DPPC/HEMA-AAm films against temperature; three of their surface micrographies are showed (27, 31 and 45 °C).

In Figure 5 is possible to visualize roughness changes against sample surface temperature for DPPC/HEMA-AAm sample. This film was selected in particular to perform AFM measurements due to their background smoothness, the hydrogel does not present undulations at surface level (wrinkle morphology), this type of pattern produce molecular movement decrease with temperature increase when the surfactant is deposited on surface folds. Between 25 °C and 29 °C, a slight roughness decrease is detected, change that could be related to small inclinations of surfactant molecules – hydrocarbon chains melting and minimal interdigitation – favoring surface smoothness (L_c-$L_{\beta'}$ transition and $L_{\beta'}$ phase). At 31 °C a local maximum is reached, this behavior

should be related to a bilayer tilting process ($L_{\beta'}$-$P_{\beta'}$ transition). Between 33 °C and 37 °C, ripple phase ($P_{\beta'}$, metastable) is visualized. Posteriorly, an abrupt roughness variation is detected, changes that are associated to a phase transition ($P_{\beta'}$-L_{α}). Past 44 °C and until 50 °C, L_{α} phase could be possibly observed, this state is related to an important roughness decrease, phenomenon linked to molecule movement and to structural reorganization at surface level. In general, when the temperature increase, the interactions between DPPC molecules becomes lower, producing bilayer disintegration, leading to a smooth surface. Similar thermal behavior, roughness evolution and AFM micrographies were obtained by Oncins et al., 2007.

The following tables summarize the results related to dimensions of crystals, for the case of HEMA-DEGDMA and HEMA-AAm compounds (Table 1), and parameters of undulated patterns, for the case of HEMA-PEGDA$_{575/700}$ (Table 2). In the first table is possible to observe that both techniques measure similar dimensions for the crystals, except for the square-like crystals on the sample HEMA-AAm using AFM technique, in where the measured lengths and widths were considerably lower than FE-SEM. This indicate that is not possible to asseverate that crosslinking agent produce an important difference in crystal morphology or sizes.

Table 1. Dimensions of the crystals formed at the surface of HEMA-DEGDMA and HEMA-AAm films using different techniques.

Crosslinking agent	Technique	Rod-like Crystals / µm	Square-like Crystals / µm
DEGDMA	FE-SEM	6.92 ± 2.62 (L) 0.86 ± 0.47 (W)	5.78 ± 0.91 (L) 3.07 ± 0.49 (W)

	AFM	-	5.27 ± 0.46 (L)
		-	2.56 ± 0.31 (W)
		-	0.33 ± 0.03 (H)
AAm	FE-SEM	4.16 ± 0.21 (L)	13.83 ± 3.67 (L)
		2.53 ± 0.19 (W)	12.51 ± 2.04 (W)
	AFM	-	3.84 ± 0.20 (L)
		-	2.69 ± 0.14 (W)
		-	0.32 ± 0.02 (H)

(L): Large, (W): Width and (H): Height of the crystal.

Different is the case for the samples HEMA-PEGDA$_{575/700}$ that present undulations at surface level (Table 2), in where the wave amplitude and wavelength of the undulations are similar for the main and secondary chains measured with FE-SEM and AFM techniques. In general, the dimensions of the main chain are twice as than that of the secondary chain. Also is possible to recognize a tendency related to crosslinking agent nature, when molecular weight increase, both parameters (amplitude and wavelength) also increase.

Table 2. Comparison of wrinkled pattern parameters (wave amplitude and wavelength) for HEMA-PEGDA$_{575/700}$ using FE-SEM and AFM.

Crosslinking agent	Technique	Main Chain / µm	Secondary Chain / µm
PEGDA$_{575}$	FE-SEM	4.31 ± 0.47 (w)	2.67 ± 0.24 (w)
	AFM	4.68 ± 0.36 (w)	2.35 ± 0.31 (w)
		0.95 ± 0.13 (A)	0.56 ± 0.12 (A)

$PEGDA_{700}$	FE-SEM	5.78 ± 0.47 (w)	3.48 ± 0.42 (w)
	AFM	6.05 ± 0.69 (w)	3.16 ± 0.71 (w)
		1.31 ± 0.20 (A)	0.88 ± 0.11 (A)

(w): Wavelength and (A): Amplitude of the undulations.

- *Ellipsometric Measurements.*

The different refractive indexes were measured through an Abbe refractometer, these values were: 1.445 for HEMA-DEGDMA, 1.442 for HEMA-$PEGDA_{575}$, 1.448 for HEMA-$PEGDA_{700}$, 1.425 for HEMA-AAm and 1.546 for DPPC.

Hydrogel films were hydrated with distilled water by immersion/emersion of the substrate at 0.01 mm/s using the dip coating technique (wetting take near to 30 min., emulating the conditions of DPPC deposition), this procedure is only performed once time in the beginning of the thermo-ellipsometry study. Thus, polymer thickness variation was associated to water release or molecular movement, these changes were studied using three consecutive heating cycles. Then, over the same bare hydrogel film, DPPC bilayer was deposited. Three subsequent temperature cycles were applied to the sample with a heating ramp of 0.2 °C per minute. At every Celsius degree, thirty data were obtained; mean thickness value and standard deviation were used as thickness and associated error for each point. In this way, the data plotted in Figures 6-8 were obtained.

Figure 6a shows the ability of HEMA-DEGDMA hydrogel films for release water when it is subjected to external temperature changes. Thus, in the first thermal cycle, specifically in the interval among 18.5 °C and 55.0 °C, a slight thickness decrease was detected. In this zone, hydrogel thickness varied between 279.7 nm and 264.2 nm with a total thickness variation of 15.5 nm. When the system was heated again (second

thermal cycle) a lower thickness variation was detected (9.4 nm), demonstrating that some water remains into the hydrogel film, the third thermal cycle present similar behavior with lower thickness variation (4.0 nm). Therefore, after the three heating cycles, there was no water remaining to be released. In addition, this thickness change could be associated to polymer molecular movements promoted by thermodynamical system changes.

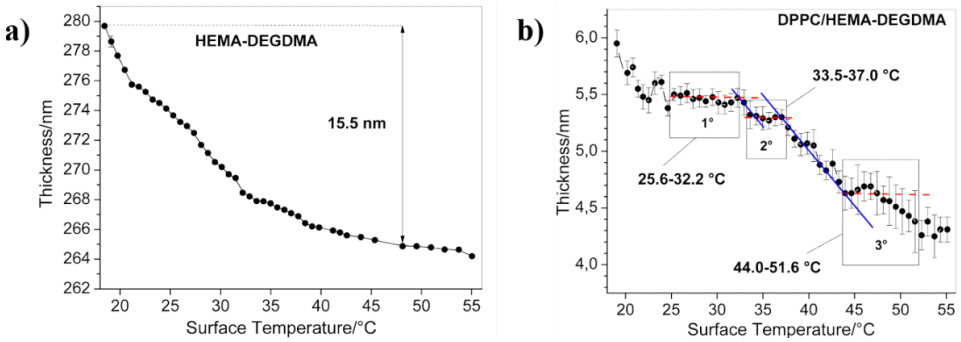

Figure 6. Ellipsometric studies during the first heating cycle of the systems: a) HEMA-DEGDMA and b) DPPC/HEMA-DEGDMA.

DPPC/HEMA-DEGDMA system (Figure 6b) show three clear plateaus during its first thermal cycle, these were located between 25.6-32.2 °C ($L_{\beta'}$ phase), 33.5-37.0 °C ($P_{\beta'}$ phase), 44.0-51.6 °C (order) and 52.3-55.1 °C (disorder) (L_{α} phase), with their respective transitions: 19.0-24.6 °C (L_c-$L_{\beta'}$), 32.9-33.4 °C ($L_{\beta'}$-$P_{\beta'}$) and 37.7-43.3 °C ($P_{\beta'}$-L_{α}). The L_{α} phase present a decrease in layer thickness coupled with a high associated error explained by the disorder of the hydrocarbon chains at this temperature. Subsequent measures (second and third thermal cycles) show similar

behavior but showing more diffuse or less defined phases.

Figure 7a show small thickness variation near to 1.8 nm when HEMA-PEGDA$_{575}$ system was heated between 22.7-55.0 °C. First, second and third heating cycles show a continuous decrease in their total thickness variation, similar behavior than HEMA-DEGDMA hydrogel films (Figure 6a) but in larger amounts than the last one (15.5 nm > 1.8 nm). This effect could be related to hydrogel topography, small faceted clusters prevent water release due to occlusion into highly packed polymer networks (Figure 2a).

The system composed by DPPC/HEMA-PEGDA$_{575}$ hydrogel films show a total decrease in thickness values from 5.6 to 5.0 nm between 23.4 °C and 55.0 °C (Figure 7b). Three phases were detected: 26.6-28.0 °C ($L_{\beta'}$ phase), 32.2-35.6 °C ($P_{\beta'}$ phase) and 45.3-55.2 °C (L_{α} phase, 45.3-52.3 °C (order) and 53.4-55.2 °C (disorder)), with their respective transitions: 23.4-26.0 °C (L_c-$L_{\beta'}$), 28.7-31.5 °C ($L_{\beta'}$-$P_{\beta'}$) and 36.3-44.6 °C ($P_{\beta'}$-L_{α}). It is important to highlight that thickness increase is associated to $L_{\beta'}$-$P_{\beta'}$ transition, this results are in agreement with previously reported values (Stamatoff et al., 1982).

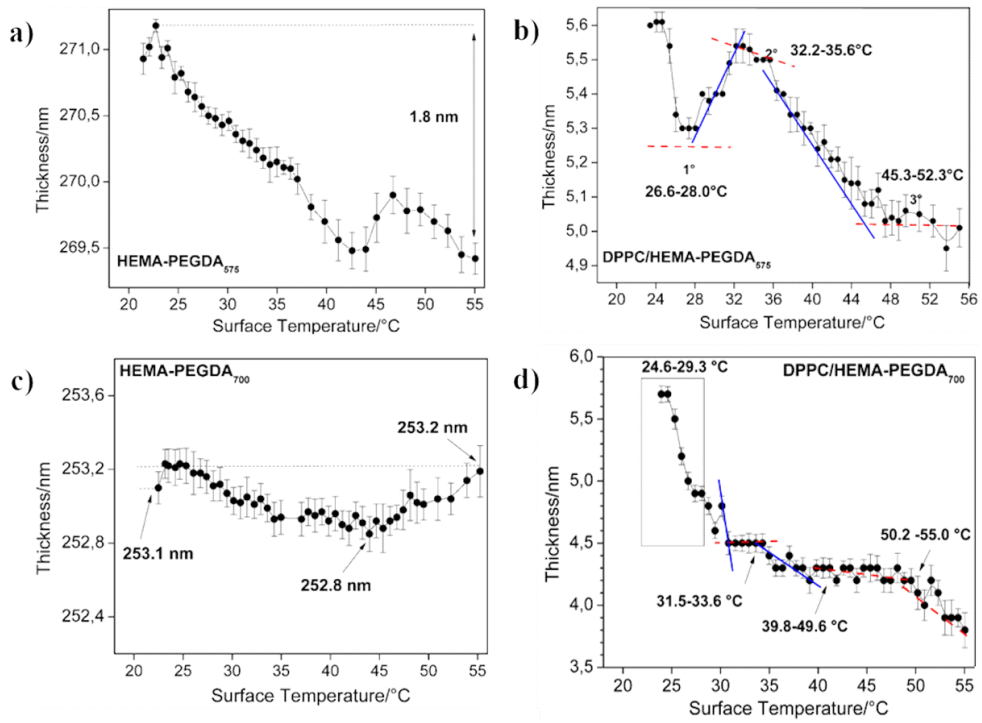

Figure 7. Ellipsometric studies during the first heating cycle of the systems: a) HEMA-PEGDA$_{575}$, b) DPPC/HEMA-PEGDA$_{575}$, c) HEMA-PEGDA$_{700}$ and d) DPPC/HEMA-PEGDA$_{700}$.

A maximum thickness change of 0.3 nm was detected during the first thermal cycle

(between 22.5 °C and ~ 45 °C) for the sample HEMA-PEGDA$_{700}$ (Figure 7c), this results clearly shows that this system is inefficient for water delivery, possibly due to its high crosslinking degree (Figure 2b), disfavoring molecular movements of the polymeric chains arrangement. Figure 7d showed a total thickness decrease from 5.7 to 3.8 nm when the DPPC was deposited as bilayer over the hydrogel. The artificial membrane was heated between 23.8 and 55.0 °C. At high temperatures, DPPC molecules were found to be highly tilted, losing their bilayer structure and characteristics. In this graph, only the first thermal cycle is shown, with two clear plateaus located between 31.5-33.6 °C and 39.8-55.0 °C (39.8-49.6 °C L_α ordered and 50.2-55.0 °C L_α disordered). This temperature range determine $P_{\beta'}$ and L_α phases limits respectively, with their respective phase transitions. Additionally, between 24.6-29.3 ° C is not possible to separate L_c-$L_{\beta'}$ and $L_{\beta'}$, probably due to roughness of the hydrogel surface.

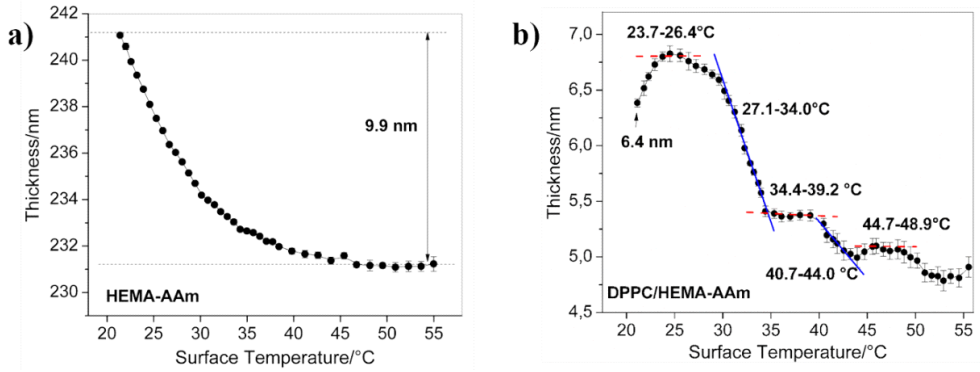

Figure 8. Ellipsometric studies during the first heating cycle of the systems: a) HEMA-

AAm and b) DPPC/HEMA-AAm.

The HEMA-AAm hydrogel film (Figure 8a) present a clear thickness decrease from 241.1 nm to 231.1 nm when is heated between 21.3 °C and 55.0 °C - typical behavior related to water release - similar tendency is shown in Figure 6a. On the other hand, Figure 8b show DPPC thermal behavior deposited over HEMA-AAm film, whose initial value is 6.4 nm at 21.0 °C; the layer thickness increase until reach the first plateau between 23.7 and 26.4 °C ($L_{\beta'}$ phase). Over this temperature a decrease is observed from 27.1 °C to 34.0 °C, whose thickness difference is 1.1 nm attributed to phase transition $L_{\beta'}$- $P_{\beta'}$. Between 34.4 °C and 39.2 °C a second plateau is showed, possibly corresponding to $P_{\beta'}$ phase (Stamatoff et al., 1982). Posteriorly, over 40.7 °C until 44.0 °C a slight thickness decrease, attributed to $P_{\beta'}$-L_{α} transition, is observed. Finally, at higher temperatures, two different fluid phases were detected; L_{α} (ordered) from 44.7 °C to 48.9 °C and L_{α} (disordered) from 49.4°C to 55.4 °C (Leonenko et al., 2004).

Several phases have been identified according to DPPC bilayer models, where the higher-temperature phases are characterized by an increase of lateral motions of the molecules enhancing hydrocarbon chain overlapping (interdigitation) (Yeagle, 2005). Other research groups also study the thermotropic behavior of supported DPPC bilayer, thus thickness values for gel phase was 5.2–5.4 nm (Yarrow et al., 2011), result that is slightly lower compared to other studies, but in reasonable agreement with reported values (using AFM) of 5.8–5.9 nm (Rinia et al., 2000), 5.6 nm (Mou et al., 1996) or 6.35 nm for a full hydrated DPPC bilayer (Nagle and Tristram-Nagle, 2000). However, values obtained for fluid phase (3.8 ± 0.4 nm) are comparable to 3.6 nm (Tokomasu et al., 2003) and 3.3 nm obtained by other AFM studies (Leonenko et

al., 2004).

In our case, the total thickness difference estimated via ellipsometry technique is near to 2 nm taken from 21 to 55 °C for every sample, except for DPPC/HEMA-PEGDA$_{575}$ (Figure 7b) that present a difference of ~ 0.6 nm (significantly lower value than the obtained for other compounds). This behavior could be attributed to hydrogel characteristics (hydrophilic wrinkles morphology, Figure 2a). Their compact corrugated topography present large amount of defects, according to this, DPPC bilayer is found exclusively organized in regions of low curvature, with their mayor axes aligned preferentially along the directions of the striations of the buckled topography, therefore the deposition of the surfactant closely follows the scaffold morphology (Gilmore et al., 2011). Thus, DPPC essentially lose fluidity and, also, the ability to tilt the molecules within bilayer environment. Stability and structural integrity were studied by different research groups through the combination of electrostatic, hydration and Van der Walls interactions between surfactant molecules (Cremer and Boxer, 1999). Others research groups described a structural instability leading to collapse of a single (biphasic) phospholipid bilayer at the solid-liquid interface triggered by thermal annealing (Gilmore et al., 2014). In the Table 3 are summarized the phases and phase transitions temperatures, measured through Ellipsometry and AFM, for DPPC bilayers deposited over different hydrogels films used as scaffold. These results show that, in general, all the samples present similar thermal behavior when a DPPC bilayer is deposited over the different hydrogels, but through ellipsometry plots is possible to asseverate that DEGDMA and AAm based compounds produce intense phase transitions compared to PEGDA based hydrogels, indicating that this last reactive is not appropriate to be used in the scaffold mixture due to their

high crosslinking degree.

Table 3. Comparison of phase and phase transition temperatures measured with Ellipsometry and AFM for different hydrogel films used as scaffold.

	DPPC Phases and Phase transitions (°C)					
Hydrogel Scaffold	**L_c-$L_{\beta'}$**	**$L_{\beta'}$**	**$L_{\beta'}$ - $P_{\beta'}$**	**$P_{\beta'}$**	**$P_{\beta'}$-L_α**	**L_α**
HEMA-DEGDMA[a]	19.0-24.6	25.6-32.2	32.9-33.4	33.5-37.0	37.7-43.3	44.0-55.1
HEMA-PEGDA$_{575}$[a]	23.4-26.0	26.6-28.0	28.7-31.5	32.2-35.6	36.3-44.6	45.3-55.2
HEMA-PEGDA$_{700}$[a]	24.6-29.3		30.0-30.9	31.5-33.6	34.2-39.2	39.8-55.0
HEMA-AAm[a]	-	23.7-26.4	27.1-34.0	34.4-39.2	40.7-44.0	44.7-55.4
HEMA-AAm[b]	25.0-29.0		29.0-33.0	33.0-37.0	37.0-44.0	44.0-55.0

a: Ellipsometry and b: AFM.

Finally, according to ellipsometry results, the average layer thickness above 35 °C decrease by ~11–25 % (taken as initial and final temperature ~21 °C and 37 °C, respectively). This percentage variation is higher in the fluid phase, values that are related with changes in the molecular organization such as: interdigitation, disorder of their chains, etc.

- **Conclusions**

Over a cleaned and hydrophilic silicon wafer surface, spin coating technique was used to deposit hydrogel films. Their thickness and surface homogeneity were affected by composite density/viscosity and monomers used in the reaction synthesis, among other factors. For HEMA-PEGDA$_{700}$ films, a rough surface due to the high crosslinking degree, provided by PEGDA (wrinkle patterns), was detected. Similar situation is visualized for HEMA-PEGDA$_{575}$ that present a disordered buckled surface (non-preferential wrinkles orientation) with a wider visible main chain, rounded by smaller

secondary chains connected to the main one. This corrugated structure disfavor DPPC movements and, therefore, their phases/phase transitions occurrence when system is subjected to heating cycles. In addition, the films that possess DEGDMA and AAm as crosslinking agents produce homogenous flat films with micro-crystalline structures at surface level.

Ellipsometry was proved to be an excellent tool for measure slight thickness variations in the DPPC bilayer, allowing the detection of phases/phase transitions. Ellipsometric results were consistent with complementary thermo-AFM measurements. Hydrogel scaffolds increased the DPPC stability when the system is subjected to thermal cycles, allowing the detection of ripple phases associated with a decrease in bilayer thickness, related with a certain interdigitation of the hydrocarbon chains. In general, these results proved that DPPC bilayers could be deposited homogeneously over solid substrates, forming stable systems that can resist high temperature changes without losing their conformation. More interestingly, wrinkled surface present as an excellent candidate for soft biocompatible materials with tunable surface topography.

Acknowledgments

The authors gratefully acknowledge financial support from FONDECYT Grant N° 11121281; Attraction and Insertion of Advanced Human Capital Program, PAI N° 7912010031-CONICYT. Mr. Sarabia acknowledges the financial support given by CONICYT through the Doctoral Scholarship Grant. In addition, we wish to thank the following: LNLS-Brazilian Synchrotron National Light Laboratory together with LNNano-Brazilian Nanotechnology National Laboratory for the use of FE-SEM and AFM (Brazil-Campinas) and Germany Academic Exchange Service (DAAD) due to ellipsometer equipment donation. Finally, Gwyddion development is supported by

Department of Nanometrology, Czech Metrology Institute and Roberto Villaroel Bolcis for AFM images acquisition.

References

- Andrecka, J., Spillane, K.M., Ortega-Arroyo, J., Kukura, P., 2013. Direct observation and control of supported lipid bilayer formation with interferometric scattering microscopy. ACS Nano 7, 10662–10670.

- Cremer, P.S., Boxer, S.G., 1999. Formation and Spreading of Lipid Bilayers on Planar Glass Supports. J. Phys. Chem. B 103, 2554−2559.

- Drücker, P., Gerke, V., Galla, H.J., 2014. Importance of phospholipid bilayer

integrity in the analysis of protein-lipid interactions. Biochem. Biophys. Res. Commun. 453, 143–147.

- Gilmore, S.F., Nanduri, H., Parikh, A.N., 2011. Programmed Bending Reveals Dynamic Mechanochemical Coupling in Supported Lipid Bilayers. PLoS one 6, e28517 (1–8).

- Gilmore, S.F., Sasaki, D.Y., Parikh, A.N., 2014. Thermal Annealing Triggers Collapse of Biphasic Supported Lipid Bilayers into Multilayer Islands. Langmuir 30, 4962−4969.

- González, C., Volkmann, U.G., Retamal, M.J., Cisternas, M., Sarabia, M.A., López, K.A., 2012. Thermal behavior of 1,2-dipalmitoyl-sn-3-phosphoglycerocholine bi- and multi-layers, deposited with physical vapor deposition under ellipsometric growth control. J. Chem. Phys. 136, 134709–134714.

- González-Henríquez, C.M., Pizarro-Guerra, G. del C., Sarabia-Vallejos, M.A., Rojas de la Fuente, S.D., Ulloa-Flores, M.T., Rivas-Jimenez, L.M., 2014a. In situ silver nanoparticle formation embedded into a photopolymerized hydrogel with biocide properties. J. Nanostructure Chem. 4, 119–132.

- González-Henríquez, C.M., Pizarro, G. del C., Sarabia-Vallejos, M.A., Terraza, C.A., López-Cabaña, Z.E., 2014b. In-situ preparation and characterization of silver-HEMA/PEGDA hydrogel matrix nanocomposites. Effect of crosslinking agent. Arabian J. Chem. DOI: 10.1016/j.arabjc.2014.11.012.

- González-Henríquez, C.M., Pizarro Guerra, G., Droguett-Droguett, F.A., Sarabia,

M.A., 2015a. Artificial biomembrane based on DPPC - investigation into phase transition and thermal behavior through ellipsometric techniques. Biochim. Biophys. Acta. Biomembr. 1848, 2295–2307.

- González-Henríquez, C.M., Pizarro Guerra, G., Sarabia, M.A., Terraza, C.A., 2015b. Thin and ordered hydrogel films deposited through electrospinning technique; a simple and efficient support for organic bilayers. Biochim. Biophys. Acta. Biomembr. 1848, 2126–2137.

- González-Henríquez, C.M., Sarabia-Vallejos, M.A., 2015c. Electrospinning deposition of hydrogel fibers used as scaffold for biomembranes. Thermal stability of DPPC corroborated by ellipsometry. Chem. Phys. Lipids 190, 51-60.

- Guvendiren, M., Burdick, J.A., Yang, S., 2010. Solvent induced transition from wrinkles to creases in thin film gels with depth-wise crosslinking gradients. Soft Matter 6, 5795–5801.

- Hain, N., Gallego, M., Reviakine, I., 2013. Unraveling supported lipid bilayer formation kinetics: osmotic effects. Langmuir 29, 2282–2288.

- Horcas, I., Fernández, R., Gomez-Rodríguez, J.M., Colchero, J., Gómez-Herrero, J., Baro, A.M., 2007. WSXM: A software for scanning probe microscopy and a tool for nanotechnology. Rev. Sci. Instrum. 78, 013705–8.

Hou, J., Li, Q., Han, X., Lu, C., 2014. Swelling/Deswelling-Induced Reversible Surface Wrinkling on Layer-by-Layer Multilayers. J. Phys. Chem. B 118, 14502–14509.

- Huang, R., 2005. Kinetic wrinkling of an elastic film on a viscoelastic substrate. J.

Mech. Phys. Solids 53, 63–89.

- Jing, Y., Trefna, H., Persson, M., Kasemo, B., Svedhem, S., 2014. Formation of supported lipid bilayers on silica: relation to lipid phase transition temperature and liposome size. Soft Matter 10, 187–195.

- Kim, B.H., Choi, Y., Kim, J.Y., Shin, H., Kim, S., Son, S.W., Kim, S.O., Kim, P., 2014. Wrinkle-Directed Self-Assembly of Block Copolymers for ligning of Nanowire Arrays. Adv. Mater. 26, 4665–4670.

- Klapetek, P., Valtr, M., Nečas, D., Salyk, O., Dzik, P., 2011. Atomic force microscopy analysis of nanoparticles in non-ideal conditions. Nanoscale Res. Lett. 6, 514–522.

- Leonenko, Z.V., Finot, E., Ma, H., Dahms, T.E.S., Cramb, D.T., 2004. Investigation of Temperature-Induced Phase Transitions in DOPC and DPPC Phospholipid Bilayers Using Temperature-Controlled Scanning Force Microscopy. Biophys J. 86, 3783–3793.

- Luckey, M., 2014. Membrane structural biology: with biochemical and biophysical foundations. Cambridge University Press, Cambridge, U.K.

- Matsuki, H., Goto, M., Tada, K., Tamai, N., 2013. Thermotropic and Barotropic Phase Behavior of Phosphatidylcholine Bilayers. Int. J. Mol. Sci. 14, 2282–2302.

- Mou, J., Czajkowsky, D.M., Shao, Z., 1996. Gramicidin A aggregation in Supported Gel State Phosphatidylcholine Bilayers. Biochemistry 35, 3222–3226.

- Nagle, J.F., Tristram-Nagle, S., 2000. Structure of lipid bilayers. Biochim.

Biophys. Acta. Biomembr. 1469, 159–195.

- Nellis, B.A., Satcher, J. H. Jr., Risbud, S.H., 2011. Phospholipid bilayer formation on a variety of nanoporous oxide and organic xerogel films. Acta Biomater. 7, 380–386.

- Oncins, G., Picas, L., Hernández-Borrell, J., Garcia-Manyes, S., Sanz, F., 2007 Thermal Response of Langmuir-Blodgett Films of Dipalmitoylphosphatidylcholine Studied by Atomic Force Microscopy and Force Spectroscopy. Biophys. J. 93, 2713–2725.

- Palacios-Cuesta, M., Liras, M., Del Campo, A., García, O., Rodríguez-Hernández, J., 2014. Versatile Approach for the Fabrication of Functional Wrinkled Polymer Surfaces. Langmuir 30, 13244−13254.

- Rebaud, S., Maniti, O., Girard-Egrot, A.P., 2014. Tethered bilayer lipid membranes (tBLMs): Interest and applications for biological membrane investigations. Biochimie 107, 135–142.

- Rinia, H.A., Kik, R.A., Demel, R.A., Snel, M.M.E., Killian, J.A., Van der Eerden, J.P.J.M., De Kruijff, B., 2000. Visualization of highly ordered striated domains induced by transmembrane peptides in supported phosphatidylcholine bilayers. Biochemistry 39, 5852–5858.

- Shlomovitz, R., Schick, M., 2013. Model of a Raft in Both Leaves of an Asymmetric Lipid Bilayer. Biophys. J. 105, 1406–1413.

- Stamatoff, J., Feuer, B., Guggenheim, H.J., Tellez, G., Yamane, T., 1982.

Amplitude of Rippling in the P_β Phase of Dipalmitoylphosphatidylcholine Bilayers. Biophys J. 38, 217–226.

- Stiebler, R., Hoang, A.N., Egan, T.J., Wright, D.W., Oliveira, M.F., 2010. Increase on the Initial Soluble Heme Levels in Acidic Conditions Is an Important Mechanism for Spontaneous Heme Crystallization In Vitro. PloS one 5, e12694 (1–9).

- Thiam, A.R., Farese, R.V. Jr., Walther, T.C., 2013. The biophysics and cell biology of lipid droplets. Nat. Rev. Mol. Cell Biol. 14, 775–786.

- Tidswell, I.M., Ocko, B.M., Pershan, P.S., Wasserman, S.R., Whitesides, G.M., Axe, J.D., 1990. X-ray specular reflection studies of silicon coated by organic monolayers (alkylsiloxanes). Phys. Rev. B 41, 1111–1128.

- Tokumasu, F., Jin, A.J., Feigenson, G.W., Dvorak, J.A., 2003. Atomic force microscopy of nanometric liposome adsorption and nanoscopic membrane domain formation. Ultramicroscopy 97, 217–227.

- Tokudome, Y., Suzuki, K., Kitanaga, T., Takahashi, M., 2012. Hierarchical Nested Wrinkles on Silica−Polymer Hybrid Films: Stimuli-Responsive Micro Periodic Surface Architectures. Sci. Rep. 2, 683 (1−6).

- Watkins, E.B., Miller, C.E., Liao, W.P., Kuhl, T.L., 2014. Equilibrium or quenched: fundamental differences between lipid monolayers, supported bilayers, and membranes. ACS Nano 8, 3181–3191.

- Yarrow, F., Kuipers, B.W.M., 2011. AFM study of the thermotropic behaviour of

supported DPPC bilayers with and without the model peptide WALP23. Chem. Phys. Lipids 164, 9–15.

- Yeagle, P.L., 2005. The Structure of Biological Membranes. CRC Press Inc., Boca Raton, USA.